Earth and Planetary Science Letters 380 (2013) 98–111

Contents lists available at ScienceDirect

Earth and Planetary Science Letters

www.elsevier.com/locate/epsl

Collision of continental corner from 3-D numerical modeling

Zhong-Hai Li [a,*], Zhiqin Xu [a], Taras Gerya [b,c], Jean-Pierre Burg [d]

[a] State Key Lab of Continental Tectonics and Dynamics, Institute of Geology, Chinese Academy of Geological Sciences, Beijing, China
[b] Institute of Geophysics, Department of Earth Sciences, ETH-Zurich, Switzerland
[c] Geology Department, Moscow State University, Moscow, Russia
[d] Geological Institute, Department of Earth Sciences, ETH and University Zurich, Switzerland

ARTICLE INFO

Article history:
Received 3 March 2013
Received in revised form 10 August 2013
Accepted 16 August 2013
Available online 9 September 2013
Editor: C. Sotin

Keywords:
continental collision
lateral extrusion
slab break-off
3-D numerical modeling
Himalaya
Zagros

ABSTRACT

Continental collision has been extensively investigated with 2-D numerical models assuming infinitely wide plates or insignificant along-strike deformation in the third dimension. However, the corners of natural collision zones normally have structural characteristics that differ from linear parts of mountain belt. We conducted 3-D high-resolution numerical simulations to study the dynamics of a continental corner (lateral continental/oceanic transition zone) during subduction/collision. The results demonstrate different modes between the oceanic subduction side (continuous subduction and retreating trench) and the continental collision side (slab break-off and topography uplift). Slab break-off occurs at a depth ($\leqslant$100 km to $\sim$300 km) that depends on the convergence velocity. The numerical models produce lateral extrusion of the overriding crust from the collisional side to the subduction side, which is also a phenomenon recognized around natural collision of continental corners, for instance around the western corner of the Arabia–Asia collision zone and around the eastern corner of the India–Asia collision zone. Modeling results also indicate that extrusion tectonics may be driven both from above by the topography and gravitational potentials and from below by the trench retreat and asthenospheric mantle return flow, which supports the link between deep mantle dynamics and shallower crustal deformation.

1. Introduction

Continental subduction and collision normally follows oceanic subduction under the combined convergent forces of 'ridge push' and/or oceanic 'slab pull' (e.g., Turcotte and Schubert, 2002). Besides the systematic geological/petrological studies of recent continental collision zones (e.g., Alpine–Zagros–Himalayan belt), analogue (e.g., Chemenda et al., 1995, 1996, 2000; Boutelier et al., 2004) and numerical models (e.g., Beaumont et al., 2001, 2009; Burov et al., 2001; Liu et al., 2004; Toussaint et al., 2004; Burg and Gerya, 2005; Sobolev and Babeyko, 2005; Gerya et al., 2008a; Yamato et al., 2007, 2008; Warren et al., 2008; Li and Gerya, 2009; Li et al., 2010, 2011; Chen et al., 2013) are also widely used and become more and more substantial to investigate continental subduction/collision processes. The numerical tectonic styles of continental subduction/collision can be either "one-sided" (overriding plate does not subduct) or "two-sided" (both plates subduct together) (Tao and O'Connell, 1992; Pope and Willett, 1998; Faccenda et al., 2008; Warren et al., 2008; Li et al., 2011). Several other possibilities such as thickening, slab drips (e.g., Toussaint et al., 2004) and slab break-off (e.g., Duretz et al., 2011, 2012; Van Hunen and Allen, 2011) have been put forward. The one-sided style can be further divided into steep (high angle) and flat (low angle) subduction/collision zones, resulting in different structures, stress states and deformation styles in the converging plates as well as different metamorphic pressure conditions of the exhumed wedge rocks (e.g., Li et al., 2011).

However, most of the models mentioned in the previous section are based on the 2-D regime, assuming that the plate is infinitely wide or that along-strike deformation in the third dimension can be neglected. 2-D models are indeed relevant to study the general processes and dynamics in the continental subduction channels and/or the interior of the continental collision zones, but far from curvilinear areas such as the continental corners. Recent 3-D numerical models of oceanic subduction, without continental collision, revealed different characteristics and scaling laws between the lateral edges and the interior of subducting slabs (e.g., Schellart et al., 2011; Li and Ribe, 2012). In nature, convergent continents have borders with transition to oceanic plates or to other continents. In addition, the corners of the natural collision zones normally have structures different from those of linear mountain belts. For example, the geological/petrological characteristics and deep structures of the western and eastern Himalayan syntaxes are very different from those of the central Himalayas (e.g. Burg et al., 1997; Burg and Podladchikov, 1999, 2000; Zeitler et al., 2001; Yin, 2006; Burg and Schmalholz, 2008; Guillot et al., 2008; Oreshin et al., 2008). Therefore, 3-D numerical

* Corresponding author.
E-mail address: Lzhhai@gmail.com (Z.-H. Li).

0012-821X/$ – see front matter
http://dx.doi.org/10.1016/j.epsl.2013.08.034

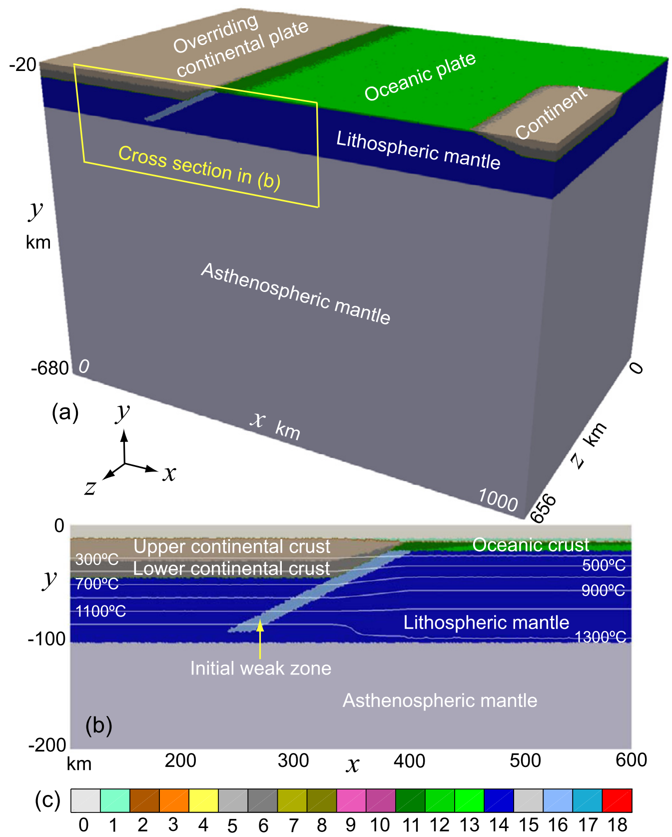

Fig. 1. Initial model configuration. (a) The 3-D model domain ($1000 \times 680 \times 656$ km) with colors indicating different rock types as in (c). The top layer ($y > -20$ km) is cut off for clarity. (b) The zoomed domain of the subduction zone as shown in (a). White lines are isotherms measured in °C. (c) The colorgrid for different rock types, with: 0-air; 1-water; 2, 3-sediment; 4-partial molten sediment; 5/6-upper/lower continental crust; 7/8-hydrated upper/lower continental crust; 9/10-partial molten upper/lower continental crust; 11/12-upper/lower oceanic crust; 13-partial molten oceanic crust; 14-lithospheric mantle; 15-asthenospheric mantle; 16/17-hydrated/serpentinized mantle; 18-partially molten mantle. The hydrated and partially molten rocks are not shown in Fig. 1, but will appear during the evolution of the model (e.g., Figs. 2 and 3). Detailed properties of different rock types are shown in Tables S2 and S3 in the supplementary Appendix.

models are necessary to investigate such three-dimensional problems (e.g., Van Hunen and Allen, 2011).

In this paper we aim investigating the dynamics during collision of continental corners by conducting 3-D high-resolution numerical simulations. After the description of numerical methodology and model setup, a series of 3-D numerical simulations with variable convergence velocities is presented. The results are then compared with the eastern Alpine–Himalayan Belt, which has involved transitions from oceanic subduction to continental collision. The comparison focuses on the occurrence and dynamics of extrusion tectonics around the western corner of the Arabia–Asia collision zone (e.g., McClusky et al., 2000; Sengor et al., 2005) and around the eastern corner of the India–Asia collision zone (e.g., Wang et al., 2001; Zhang et al., 2004). In addition, several important processes such as break-off of the oceanic slab, asthenospheric mantle return flow, and topography evolution in the 3-D collisional processes are discussed.

2. 3-D numerical modeling method

2.1. Numerical setup and boundary conditions

Large scale models ($1000 \times 680 \times 656$ km, Fig. 1) are designed for the study of dynamic processes during continental corner collision involving subduction of the lithospheric mantle. The Cartesian spatial domain is resolved by $501 \times 341 \times 165$ grid points with the resolution of 2×2 km in the x–y plane and 4 km in the along-strike z-direction. The lithological structure of the model is represented by a dense grid of about 330 million randomly distributed markers used for advecting various material properties and temperatures.

The velocity boundary conditions are free slip at the top ($y = 0$) and at both the front and back boundaries ($z = 0$ and 656 km). The left and right boundaries ($x = 0$ and 1000 km) use constant normal velocities (convergence) in x-direction, which define the material influx through these side walls. For the permeable lower boundary condition (e.g., Burg and Gerya, 2005; Gerya et al., 2008a; Li et al., 2010), an external outflux boundary implies constant normal velocity and zero shear stress conditions to be satisfied at ∼200 km below the base of the model domain. The external boundary condition allows global conservation of mass in the computational domain and is implemented by using the following limitation for velocity components at the lower boundary: $\partial V_x/\partial y = 0$, $\partial V_z/\partial y = 0$, $\partial V_y/\partial y = (V_{y_{\text{external}}} - V_y)/\Delta y_{\text{external}}$, where $\Delta y_{\text{external}}$ is the vertical distance from the lower boundary to the external boundary and $V_{y_{\text{external}}}$ is the constant normal velocity on the external boundary.

2.2. Material and thermal configuration

In the initial model setup, the overriding plate is homogeneous continent in the transverse z-direction. The subducting plate is composed of half continental (328 km wide) and half oceanic (328 km wide) lithospheres in z-direction (Fig. 1a), behind the oceanic-only subducting plate (656 km in z-direction and 500 km in x-direction). In the vertical section of the continental side (Fig. 1a and 1b) the initial material setup implies the 3-D transition from oceanic subduction to continental collision, which is similar to that of previous 2-D models (e.g., Gerya et al., 2008a; Li and Gerya, 2009; Li et al., 2011, 2012). In the continental domain, the initial material field incorporates a 35 km thick continental crust composed of 20 km upper crust and 15 km lower crust, resting on the 58 km lithospheric mantle and the subjacent 575 km asthenospheric mantle. The oceanic domain is comprised of an 8 km thick oceanic crust overlying the 82 km thick lithospheric mantle and the subjacent 575 km asthenospheric mantle. The viscous flow law of 'wet quartzite' describes the behavior of both the sediment and continental upper crust, while the 'Plagioclase An_{75}' represents the continental lower crust and the oceanic crust (Tables S2 and S3; Ranalli, 1995). Subduction initiation is imposed along a ∼10 km thick weak zone dipping ∼25° in the lithospheric mantle. This weak zone has a 'wet olivine' rheology in contrast to the 'dry olivine' rheology elsewhere in both the lithospheric and asthenospheric mantle. The rheological properties of hydrated and partially molten crustal and mantle rocks are shown in Tables S2 and S3.

The top surface of the lithosphere is calculated dynamically as an essentially internal free surface by using a buffer layer of 'sticky air' (Gerya and Yuen, 2003; Schmeling et al., 2008; Crameri et al., 2012). It is an initially 12–15 km thick layer above the upper crust, which changes dynamically during experiments. The composition is either "air" (1 kg/m^3, above $y = -12$ km water level) or "water" (1000 kg/m^3, below $y = -12$ km water level), which has a low viscosity (10^{19} Pa s). Crameri et al. (2012) found that the sticky air approach is adequate as long as the term $(\eta_{st}/\eta_{ch})/(h_{st}/L)^3$ is small, where η_{st} and h_{st} are the viscosity and thickness of the sticky air layer, and η_{ch} and L are the characteristic viscosity and length scale of the model, respectively. According to this criterion, the quality of the internal free-surface condition in our models is rather moderate. But further decrease